

Revisiting falloff curves of thermal unimolecular reactions

J. Troe and V. G. Ushakov

Citation: *J. Chem. Phys.* **135**, 054304 (2011); doi: 10.1063/1.3615542

View online: <http://dx.doi.org/10.1063/1.3615542>

View Table of Contents: <http://jcp.aip.org/resource/1/JCPSA6/v135/i5>

Published by the [American Institute of Physics](#).

Additional information on *J. Chem. Phys.*

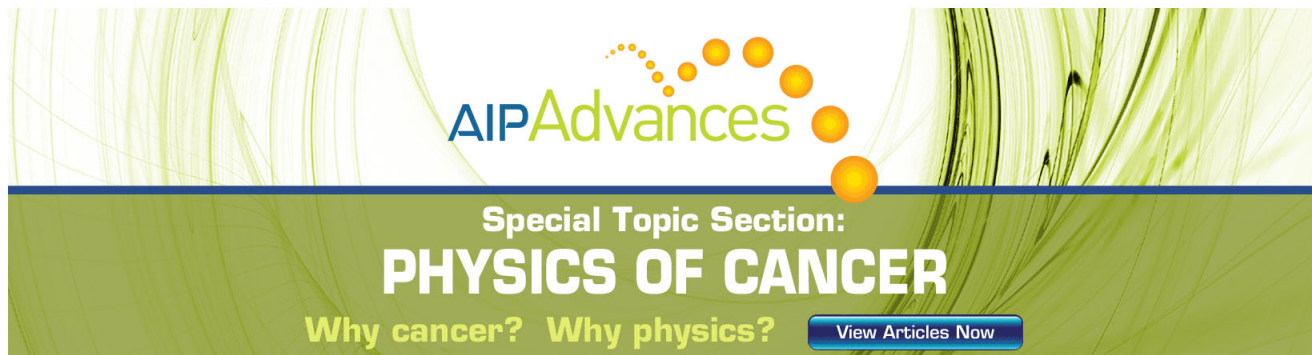
Journal Homepage: <http://jcp.aip.org/>

Journal Information: http://jcp.aip.org/about/about_the_journal

Top downloads: http://jcp.aip.org/features/most_downloaded

Information for Authors: <http://jcp.aip.org/authors>

ADVERTISEMENT



AIPAdvances

Special Topic Section:
PHYSICS OF CANCER

Why cancer? Why physics? [View Articles Now](#)

Revisiting falloff curves of thermal unimolecular reactions

J. Troe^{1,2,a)} and V. G. Ushakov³

¹*Institute for Physical Chemistry, University of Göttingen, Tammannstrasse 6, D-37077 Göttingen, Germany*

²*Max-Planck-Institute for Biophysical Chemistry, Am Fassberg 11, D-37077 Göttingen, Germany*

³*Institute of Problems of Chemical Physics, Russian Academy of Sciences, 142432 Chernogolovka, Russia*

(Received 16 April 2011; accepted 30 June 2011; published online 1 August 2011)

Master equations for thermal unimolecular reactions and the reverse thermal recombination reactions are solved for a series of model reaction systems and evaluated with respect to broadening factors. It is shown that weak collision center broadening factors F_{cent}^{wc} can approximately be related to the collision efficiencies β_c through a relation $F_{cent}^{wc} \approx \max\{\beta_c^{0.14}, 0.64(\pm 0.03)\}$. In addition, it is investigated to what extent weak collision falloff curves in general can be expressed by the limiting low and high pressure rate coefficients together with central broadening factors F_{cent} only. It is shown that there cannot be one “best” analytical expression for broadening factors $F(x)$ as a function of the reduced pressure scale $x = k_0/k_\infty$. Instead, modelled falloff curves of various reaction systems, for given k_0 , k_∞ , and F_{cent} , fall into a band of about 10% width in $F(x)$. A series of analytical expressions for $F(x)$, from simple symmetric to more elaborate asymmetric broadening factors, are compared and shown to reproduce the band of modelled broadening factors with satisfactory accuracy. © 2011 American Institute of Physics. [doi:10.1063/1.3615542]

I. INTRODUCTION

The pressure dependence of thermal unimolecular dissociation and the reverse thermal recombination reactions is of large fundamental and practical importance such that it continues to receive considerable attention. In the framework of the Lindemann-Hinshelwood (LH) model of unimolecular reactions (see, e.g., Ref. 1) it is characterized by a pseudo-first order rate constant for dissociation

$$k = Z[M]k^*f^*/(Z[M] + k^*), \quad (1.1)$$

which with varying reaction order, depends on the bath gas concentration $[M]$ and hence on the pressure. It changes from a limiting low pressure second order rate constant $k_0 = Z[M]f^*$ (where $Z[M]$ denotes the collision frequency for energy transfer and f^* is the equilibrium population of reactive states) to a limiting high pressure first order rate constant $k_\infty = k^*f^*$ (where k^* denotes the first order rate constant for dissociation of reactive states). In doubly reduced form, i.e., with k/k_∞ as a function of the $[M]$ - and, hence, pressure-proportional ratio $x = k_0/k_\infty$, the “falloff” expression of the rate constant given by Eq. (1.1) alternatively can be written as

$$k/k_\infty = x/(1+x) = F_{LH}(x) \quad (1.2)$$

with a “Lindemann-Hinshelwood factor” $F_{LH}(x)$. The pressure dependence thus is expressed by the ratio of the two parameters k_0 and k_∞ .

It is well known that more detailed unimolecular rate theory leads to a broadening of the reduced falloff curves which can be represented in the form²

$$k/k_\infty = F_{LH}(x)F(x) \quad (1.3)$$

with a “broadening factor” $F(x) = F^{sc}(x)F^{wc}(x)$ composed of strong collision and weak collision broadening factors, $F^{sc}(x)$ and $F^{wc}(x)$, respectively. The former can be calculated when Eq. (1.1) is replaced by an expression which takes into account the energy (E)- and angular momentum (quantum number J)-dependences of k^* and f^* in Eq. (1.1) through

$$k = \sum_{J=0}^{\infty} (2J+1) \int_{E_0(J)}^{\infty} Z[M]k(E, J)f(E, J) \times dE / \{Z[M] + k(E, J)\} \quad (1.4)$$

Here, $E_0(J)$ denotes the threshold energy for dissociation, $f(E, J)$ are the equilibrium populations, and $k(E, J)$ are the specific rate constants for dissociation.

The evaluation of a large number of rigid activated complex RRKM (Rice-Ramsperger-Kassel-Marcus) calculations of k for a variety of reaction systems^{2,3} has suggested that $F^{sc}(x)$ in the simplest way can be approximated by

$$F^{sc}(x) \approx (F_{cent}^{sc})^{1/[1+(\log x/N^{sc})^2]} \quad (1.5)$$

with a “center broadening factor” F_{cent}^{sc} and a width parameter

$$N^{sc} \approx 0.75 - 1.27 \log F_{cent}^{sc} \quad (1.6)$$

related to F_{cent}^{sc} . Allowing for further complexity, asymmetry corrections of Eq. (1.5) were also elaborated.^{2,3} Since the proposition of Eq. (1.5), a series of alternative falloff expressions have been proposed (see, e.g., Refs. 4–15). Nevertheless, Eq. (1.5) has proven most convenient for representing experimental and theoretical results and is widely used in gas phase kinetics (see, e.g., the combustion and atmospheric chemistry data bases^{16–18}).

Explicit solutions of master equations of unimolecular reactions with the aim to obtain weak collision broadening factors $F^{wc}(x)$ in the falloff range have been much less

^{a)} Author to whom correspondence should be addressed. Electronic mail: shoff@gwdg.de.

frequent.^{2,19,20} In order to account for weak collision effects, one might be tempted to multiply the collision frequency Z in Eq. (1.4) by a collision efficiency β_c which is smaller than unity. The result of this approach would be a neglect of weak collision broadening, i.e., $F^{wc}(x) = 1$. The analysis of solutions of the master equation, however, has shown that this simple procedure is inadequate. The so far limited number of calculations has suggested that $F^{wc}(x)$ is smaller than unity as well and that its center value $F_{cent}^{wc} = F^{wc}(x = 1)$ decreases with decreasing collision efficiency β_c . A simple relationship

$$F_{cent}^{wc} \approx \beta_c^{0.14} \quad (1.7)$$

was obtained and some functional forms for $F^{wc}(x)$ were proposed.^{2,12} For a number of mostly technical reasons, these studies left open a number of questions, first about the general validity of Eq. (1.7), second about the form of $F^{wc}(x)$, and finally about the influence of specific molecular parameters on $F^{wc}(x)$. These questions have already been addressed nearly 30 years ago, but the required calculational effort was not invested at that time. Therefore, the present work comes back to the problem with the aim of providing practically useful and theoretically validated expressions for weak collision broadening factors.

In the second part of this work, general expressions for total broadening factors $F(x) = F^{sc}(x)F^{wc}(x)$ are considered again. The question arises, how well the pressure dependence of falloff curves can be represented by the parameters k_0 , k_∞ , and $F_{cent} = F(x = 1)$ only and how large, system-specific, deviations from such a relationship have to be expected. It does not appear very meaningful to look too much for alternative functional forms of $F(x)$ which go beyond Eqs. (1.5) and (1.6), even if weak collision contributions such as Eq. (1.7) (or the extension from the present work described later) are included. The so far available falloff calculations all suffer from simplifications; either only strong collision treatments were employed, mostly even neglecting J -dependences, or collisional energy transfer did not account for rovibrational energy transfer. Therefore, as long as calculations of the falloff curves remain only approximate, simple expressions such as Eqs. (1.5) and (1.6), and their asymmetry extensions such as proposed in the present work, continue to have their justification.

II. SOLUTION OF THE MASTER EQUATION

In general form the rate constant k is given by

$$k = \sum_{J=0}^{\infty} (2J+1) \int_{E_0(J)}^{\infty} k(E, J) h(E, J) f(E, J) dE, \quad (2.1)$$

where $h(E, J)$ denotes a non-equilibrium population factor. For strong collisions, according to Eq. (1.4), $h(E, J)$ has the form

$$h^{sc}(E, J) = Z[M] / \{Z[M] + k(E, J)\} \quad (2.2)$$

at $E \geq E_0(J)$, while it is unity at $E < E_0(J)$. Along the falloff curve, for $E \geq E_0(J)$, $h^{sc}(E, J)$ increases from $Z[M]/k(E, J)$ at the low pressure limit to unity at the high pressure limit. In

order to obtain $h(E, J)$ for weak collisions, the full master equation of the unimolecular reaction needs to be solved. Besides $k(E, J)$, this also requires information on the collisional energy transfer transition probabilities $P(E', J'; E, J)$ from (E, J) to (E', J') , as well as the total energy transfer frequency per unit concentration $Z(E, J)$.

In the following we restrict ourselves to an exponential collision model on the energy scale using²²

$$P(E', E) = \frac{1}{\alpha + \gamma} \begin{cases} \exp[(E - E')/\alpha] \text{ for } E' < E \\ \exp[(E' - E)/\gamma] \text{ for } E' \geq E \end{cases} \quad (2.3)$$

with the two parameters α and γ , see below. Under steady-state conditions, for not too high temperatures (say $E_0/kT > 10$), and extending the lower limit of the energy scale to $-\infty$, the master equation in continuous form then can be transformed into the corresponding integral equation for the non-equilibrium factor

$$h(E) \approx \frac{Z[M]}{Z[M] + k(E)} \int_{-\infty}^{\infty} P(E, E') h(E') dE'. \quad (2.4)$$

Solving this equivalent of the steady-state master equation leads to $h(E)$ and through Eq. (2.1) to the rate constant k . In the following we describe several methods to solve Eq. (2.4), see also Refs. 19–22. After this, we summarize our results for $h(E)$ and $F(x)$.

One way to solve the integral Eq. (2.4) is an iterative procedure. One inserts a trial function $h^{(0)}(E)$ into the right-hand side of the equation, obtains a first approximation $h^{(1)}(E)$ which again is inserted into the right-hand side, and so on. This method was originally used in Ref. 2 and led to Eq. (1.7). A series of different algorithms in the meantime were applied in other work (see, e.g., Refs. 23 and 24, and work cited therein), mostly employing exponential down collision models which are similar but not identical with the present overall exponential model of Eq. (2.3).

In the present work we have chosen two methods to solve Eq. (2.4) which we briefly characterize in the following. Before we do this, a number of transformations of equations and parameters appear appropriate. As stated before, we restrict ourselves to a 1D-exponential collision model on the energy scale only. However, we retain the J -dependence in the employed $k(E, J)$ and $E_0(J)$ for the calculation of the final rate constant. The nonequilibrium factors $h(E)$ are thus calculated relative to the $E_0(J)$ (denoted by E_0). The parameters α and γ in Eq. (2.3) are linked by detailed balancing. Following the simplification suggested in Ref. 22, this is accounted for by using

$$1/\gamma = 1/\alpha + 1/F_E kT \quad (2.5)$$

with F_E defined through

$$F_E = \frac{\sum_{J=0}^{\infty} (2J+1) \int_{E_0(J)}^{\infty} f(E, J) dE}{\sum_{J=0}^{\infty} (2J+1) f(E_0(J)) kT} \quad (2.6)$$

in order to characterize the energy dependence of the rovibrational density of states $\rho(E, J)$ in an averaged way. The equilibrium population $f(E, J)$ here is expressed by

$$f(E, J) = \rho(E, J) \exp(-E/kT)/Q \quad (2.7)$$

with the rovibrational partition function

$$Q = \sum_{J=0}^{\infty} (2J+1) \int_0^{\infty} \rho(E, J) \exp(-E/kT) dE, \quad (2.8)$$

$\rho(E, J)$ then is represented approximately by

$$\rho(E, J) \approx \rho(E = E_0(J), J) \exp \left\{ \frac{(F_E - 1) [E - E_0(J)]}{F_E kT} \right\}. \quad (2.9)$$

We furthermore relate the collisional parameter α in Eq. (2.3) to the collision efficiency β_c , such as obtained from the analytical solution of the master Eq. (2.4) for the low pressure limit of the reaction.²² This is done through

$$\beta_c = [\alpha/(\alpha + F_E kT)]^2, \quad (2.10)$$

which is equivalent to the relation

$$\beta_c/(1 - \beta_c^{1/2}) = -\langle \Delta E \rangle / F_E kT \quad (2.11)$$

with the average (total) energy transferred per collision $\langle \Delta E \rangle = \gamma - \alpha$. In this way, α and γ can be expressed through β_c and F_E by

$$\alpha = \beta_c^{1/2} F_E kT / (1 - \beta_c^{1/2}), \quad (2.12)$$

$$\gamma = \beta_c^{1/2} F_E kT. \quad (2.13)$$

Using these relationships, we characterize our collision model and the system temperature through the two quantities β_c and F_E .

It is well known that the integral Eq. (2.4) by differentiation can be transformed into a linear differential equation of second order which in turn is equivalent to two coupled linear differential equations of first order. With the exponential collision model these transformations lead to

$$\frac{d^2 \varphi(y)}{dy^2} - \left[\frac{\beta_c}{4} + \frac{\kappa(y)(1 - \beta_c^{1/2})}{1 + \kappa(y)} \right] \varphi(y) = 0, \quad (2.14)$$

where $y = [E - E_0(J)]/\gamma$, $\kappa(y) = k(E, J)/Z[M]$,

$$h(E) = \exp(\beta_c^{1/2} y/2) \varphi(y) / [1 + \kappa(y)]. \quad (2.15)$$

Following this, the pair of equations

$$\frac{d\varphi(y)}{dy} = \eta(y), \quad (2.16)$$

$$\frac{d\eta(y)}{dy} = \left[\frac{\beta_c}{4} + \frac{\kappa(y)(1 - \beta_c^{1/2})}{1 + \kappa(y)} \right] \varphi(y), \quad (2.17)$$

needs to be solved. One should note that $\varphi(y)$ decreases with increasing y and, for $y < 0$, it has the simple form $\varphi(y)$

$= \exp(-\beta_c^{1/2} y/2) - a^- \exp(+\beta_c^{1/2} y/2)$ which corresponds to

$$h(y) = 1 - a^- \exp(\beta_c^{1/2} y). \quad (2.18)$$

The coefficient a^- later on will be determined explicitly. One should realize that both $\varphi(y)$ and $d\varphi(y)/dy$ are continuous functions at $y = 0$ which provides matching conditions for the solutions obtained in the ranges $y < 0$ and $y > 0$.

The pair of differential Eqs. (2.16) and (2.17) can be numerically solved by standard methods. In order to obtain stable solutions, the stepwise integration should be started at large values of y and proceed towards smaller values. In the following we often refer to an auxiliary function $P(y)$ given by the root of the bracket in Eq. (2.14), i.e., by

$$P(y) = [\beta_c/4 + \kappa(y)(1 - \beta_c^{1/2})/(1 + \kappa(y))]^{1/2}. \quad (2.19)$$

As shown below, $\varphi(y)$ and $\eta(y)$ for large values of y with this function approach the values

$$\varphi(y \rightarrow \infty) \approx \exp \left[- \int^y P(y') dy' \right], \quad (2.20)$$

$$\eta(y \rightarrow \infty) = d\varphi/dy \approx -P(y)\varphi. \quad (2.21)$$

This provides a proper starting condition for the integration in the form $y^{(0)} = 20 F_E kT/\gamma$, where $\varphi(y^{(0)}) \approx 1$ and $\eta(y^{(0)}) \approx -P(y^{(0)})$. One should note that $\varphi(y)$ has a free scaling factor which later on is fixed by the matching conditions at $y = 0$. The integration is continued until $y = 0$ is reached and the matching of $h(E)$ from Eq. (2.15), by means of the derived $\varphi(y)$ and $\eta(y)$, with the solution of Eq. (2.18) for $y < 0$ can be performed. This fixes the scaling factor as $C = 2/[\varphi(y = 0) - 2\eta(y = 0)/\beta_c^{1/2}]$ and the coefficient a^- follows as

$$a^- = -[\varphi(y = 0) + 2\eta(y = 0)/\beta_c^{1/2}]/[\varphi(y = 0) - 2\eta(y = 0)/\beta_c^{1/2}]. \quad (2.22)$$

III. "SEMICLASSICAL" SOLUTION OF THE MASTER EQUATION

Although the procedure outlined in Sec. II leads to accurate numerical results for the nonequilibrium factor $h(E)$ and, hence, for the rate constant k , the alternative, approximate, solution discussed in this section provides useful additional insight and also leads to some interesting analytical relationships.

The differential Eq. (2.14) has a form which is analogous to the Schrödinger equation of quantum mechanics. One, therefore, may take advantage of the WKB (Wentzel, Kramers, Brillouin) "semiclassical" approximation to the solution of the differential equation.²⁵ For simplicity, for the present problem, we also term this solution "semiclassical". This solution of Eq. (2.14), for $y > 0$ with $P(y)$ from

Eq. (2.19), has the form

$$\varphi(y) = a^+[P(y)]^{-1/2} \exp \left[- \int_0^y P(y') dy' \right] \quad (3.1)$$

with a scaling parameter a^+ . Matching this expression at $y = 0$ to the solution of Eq. (2.18) for $y < 0$, gives

$$a^+ = 2\beta_c^{1/2}[P(y=0)]^{1/2}/[2P(y=0) + \beta_c^{1/2}], \quad (3.2)$$

$$a^- = [2P(y=0) - \beta_c^{1/2}]/[2P(y=0) + \beta_c^{1/2}]. \quad (3.3)$$

This “semiclassical” result, with Eqs. (3.2) and (3.3), reproduces the known analytical formulae for the limiting low and high pressure limits of the reaction. For $y < 0$ (i.e., $E < E_0$), in the low pressure range in particular one has²²

$$\begin{aligned} h(E) &\approx 1 - (1 - \beta_c^{1/2}) \exp[-(E_0 - E)/F_E kT] \\ &= 1 - [F_E kT / (\alpha + F_E kT)] \exp[-(E_0 - E)/F_E kT], \end{aligned} \quad (3.4)$$

while, for $y > 0$ (i.e., $E \geq E_0$), one has

$$h(E) = [Z[M]\beta_c^{1/2}/k(E)] \exp[-(E - E_0)/\alpha]. \quad (3.5)$$

On the other hand, $h(E)$ in the high pressure range approaches unity everywhere.

In spite of this good performance of the “semiclassical” solution in the limiting ranges, it does not work too well in the middle of the falloff curves. However, we worked out how this problem can be overcome. For general values of y , we replaced $P(y=0)$ in Eq. (3.2) by an average value P_{av} given by

$$P_{av}(x) = S_0(x)/y_{av}, \quad (3.6)$$

where $x = k_0/k_\infty$ as before and y_{av} is the solution of the equation

$$S_0(x) = \int_0^{y_{av}} P(y) dy \quad (3.7)$$

with

$$S_0(x) \approx 1.88 + 10.0x^{0.39}/(1 + x^{0.36}) \quad (3.8)$$

fitted by means of the numerical results of Sec. II. Then, Eqs. (3.2) and (3.3) are replaced by

$$a^+ \approx 2\beta_c^{1/2}[P_{av}(x)]^{1/2}/[2P_{av}(x) + \beta_c^{1/2}], \quad (3.9)$$

$$a^- \approx 1 - a^+/[P(y=0)]^{1/2}. \quad (3.10)$$

The quality of the so modified “semiclassical” solution of the master equation is excellent except in few exceptional cases such as demonstrated in the following model calculations. The “semiclassical” solution has the advantage of being much simpler than the full numerical treatment and, therefore, may find applications in some situations.

IV. NUMERICAL EXAMPLES: DISSOCIATION OF FORMALDEHYDE

In order to illustrate our rate constant calculations in the falloff range, we first show results for the thermal decomposition of formaldehyde H_2CO . This is a complicated reaction system with superimposed formation of molecular ($\text{H}_2 + \text{CO}$) and radical ($\text{H} + \text{HCO}$) products. As we have in hand detailed results for the sum of the specific rate constants $k(E,J)$,²⁶ we have used them for model calculations of total, strong, and weak collision broadening factors, $F_{tot}(x)$, $F^{sc}(x)$, and $F^{wc}(x)$, respectively. More detailed results for molecular vs. radical product branching fractions in the falloff range were also determined but are reported elsewhere.²⁶

We note in passing that the present calculations neglect tunnelling for the molecular channel which would lead to an additional broadening of the falloff curves, see Ref. 27. It does not appear meaningful to include tunnelling contributions into general expressions of the type of Eqs. (1.2)–(1.7), because the true limiting low pressure range may be reached only at inaccessibly low pressures; in addition, there may be leveling off at a pressure independent low pressure limit. We propose to consider falloff curves neglecting tunnelling first and then add the system-specific tunnelling contributions such as shown in Ref. 27.

Figures 1 and 2, for $\beta_c = 0.1$ and $T = 1000$ K, show the nonequilibrium factors $h(E,J=0)$ obtained at various positions x along the falloff curve. At energies below the dissociation energy $E_0(J=0)$ (here determined by the molecular channel), there is some depletion of the equilibrium population. This depletion disappears when x increases to values above unity. Only some depletion then subsists at high energies. Figure 1 (and its enlargement in Fig. 2) also illustrate the excellent agreement between the accurate, numerical (full lines) and the approximate, “semiclassical” (dashed lines) results.

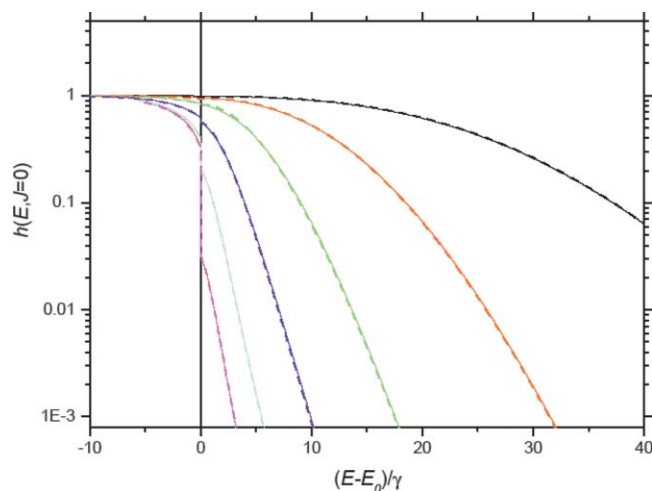


FIG. 1. Nonequilibrium population factors $h(E,J=0)$ in Eq. (2.1) for the thermal dissociation of formaldehyde at $T = 1000$ K ($F_E = 1.111$) and a weak collision efficiency $\beta_c = 0.1$ (curves from bottom to top for $x = k_0/k_\infty = 0.001, 0.01, 0.1, 1, 10, 100$, i.e., over the full falloff curve; full lines = accurate numerical results, dashed lines = approximate “semiclassical” solution of the master equation; $E_0 = E_0(J=0)$, $\gamma =$ parameter from Eq. (2.13), see text).

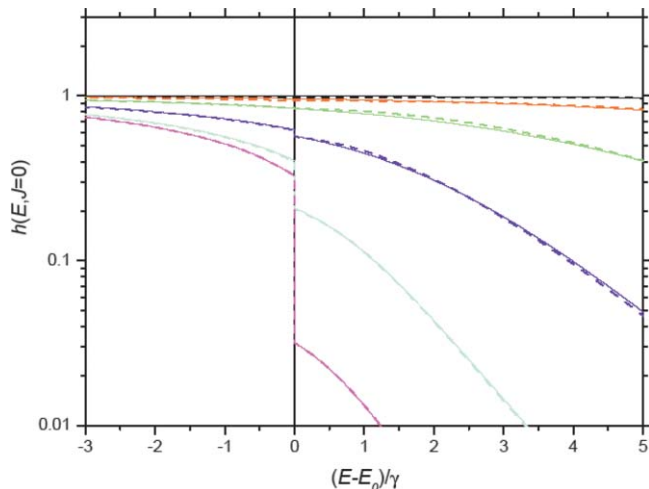


FIG. 2. As Fig. 1, but enlarged.

Total broadening factors $F_{tot}(x)$ for 1000 K, corresponding to $F_E = 1.111$, are shown in Fig. 3 for a series of collision efficiencies β_c . Obviously, there is a considerable influence of weak collisions on the shape of the total broadening factors. Again accurate, numerical (full lines) and approximate, “semiclassical” (dots) results are in excellent agreement. Next, the question arises whether the weak collision broadening factors $F^{wc}(x)$ have a similar functional form as the strong collision broadening factors $F^{sc}(x)$ such that a common expression could be used for practical applications. For example, in the simplest case one might want to approximate $F_{tot}(x)$ by

$$F_{tot}(x) \approx F_{cent}^{[1+(\log x/N)^2]^{-1}} \quad (4.1)$$

with $F_{cent} = F_{cent}^{sc} F_{cent}^{wc}$ and N given by Eq. (1.6) using F_{cent} instead of F_{cent}^{sc} . Figure 4 shows the weak collision factors $F^{wc}(x) = F_{tot}(x)/F^{sc}(x)$ contributing to Fig. 3. Although the general shapes of $F_{tot}(x)$, $F^{sc}(x)$, and $F^{wc}(x)$ look similar (increasing asymmetries for decreasing F_{cent}), there are differ-

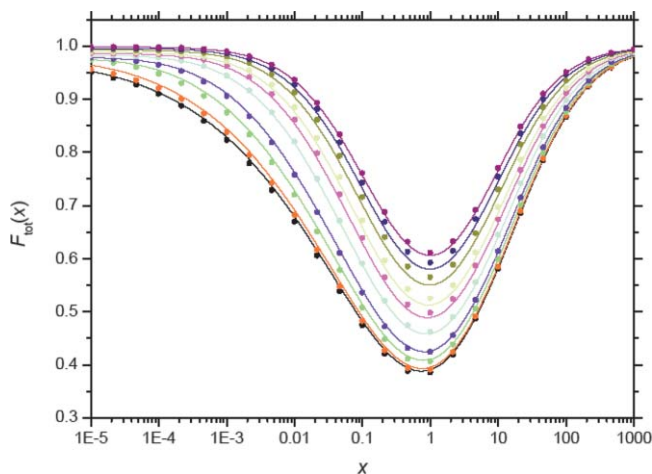


FIG. 3. Total broadening factors $F_{tot}(x)$ of the falloff curve for dissociation of formaldehyde at $T = 1000$ K and $\beta_c = 0.0001, 0.001, 0.01, 0.03, 0.1, 0.2, 0.3, 0.5, 0.7, \text{ and } 0.9$ (from bottom to top; full lines = accurate numerical results, points = approximate “semiclassical” solution of the master equation; $x = k_0/k_\infty$; see text).

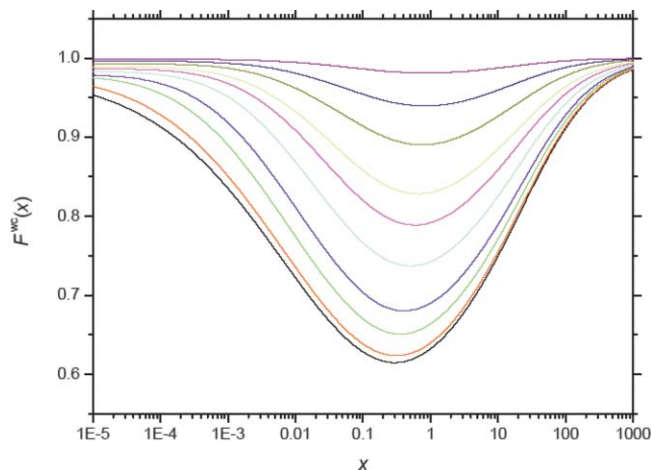


FIG. 4. Weak collision broadening factors $F^{wc}(x)$ included in $F_{tot}(x)$ from Fig. 3 (curves from bottom to top as in Fig. 3).

ences and $F_{tot}(x)$ needs not to coincide with $F^{sc}(x)$ multiplied by $F^{wc}(x)$. However, these effects are only subtle and appear negligible compared to the problem of an accurate characterization of the full strong collision falloff curve.

Finally, we inspect the dependence of F_{cent}^{wc} on the collision efficiency β_c . Again for 1000 K corresponding to $F_E = 1.111$, Fig. 5 shows the results for $F_{cent}^{wc} = F^{wc}(x=1)$ (open circles) and for the minima $F_{min}^{wc} = \min F^{wc}(x)$ (filled circles) of the slightly asymmetric broadening factors shown in Fig. 4. For $\beta_c > 0.1$, the old relationship (1.7) is well reproduced. However, we now observe a levelling of F_{cent}^{wc} and F_{min}^{wc} at smaller β_c , approaching a value F_{cent}^{wc} near 0.63. In order to see whether this levelling of F_{cent}^{wc} at small β_c , i.e., for very weak collisions, is a general phenomenon, in Sec. V we proceed to more systematic calculations of weak collision falloff curves for a series of more artificial reaction systems.

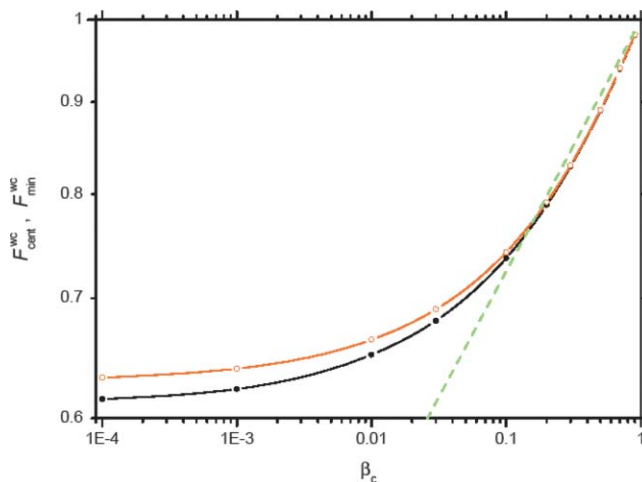


FIG. 5. Center (F_{cent}^{wc} , open circles) and minimum (F_{min}^{wc} , filled circles) weak collision broadening factors as a function of the collision efficiency β_c for the dissociation of formaldehyde at $T = 1000$ K, see Figs. 3 and 4 (the dashed line corresponds to $F_{cent}^{wc} \approx \beta_c^{0.14}$ from Eq. (1.7), see text).

V. NUMERICAL EXAMPLES: DEPENDENCE OF WEAK COLLISION BROADENING ON MOLECULAR PARAMETERS

The weak collision broadening factors $F^{wc}(x)$ in Sec. IV, for the model dissociation of formaldehyde, were shown to depend on the efficiency of collisional energy transfer such as characterized by the collision efficiency β_c . In the present section we inspect further dependences on specific molecular parameters. We design artificial molecular systems in which such parameters are varied. We consider dissociating molecules of various numbers of atoms, with various combinations of fragments, dissociation energies, rigidities of the transition states, and for different temperatures. A selection of results is documented by the figures of this section. We randomly select the frequencies of the conserved oscillators of the parent molecules and fragments between 1000 and 3000 cm^{-1} .

We consider orbiting transition states which are either completely loose (phase space theory, PST) or partially rigid with transitional mode rigidity factors $f_{rigid}(E, J)$ either of the form $f_{rigid}(E, J) \approx (1 - f_\infty) \exp[-(E - E_0(J))/c_{loose}] + f_\infty$ (simplified statistical adiabatic channel model, SSACM, of Ref. 28) or $f_{rigid} \approx \{1 + [(E - E_0(J))/c_{loose}]^2\}^{-1/2}$ (from Ref. 29). For simplicity $E_0(J)$ is taken as $BJ(J+1)$ with B related to the rotational constants of the fragments ($B = B_e$ for atom + linear (B_e) or atom + spherical top (B_e) fragments, or $B = B_1 B_2 / 2(B_1 + B_2)$ for top (B_1) + top (B_2) fragments). We first illustrate the influence of the rigidity of the transition states in Figs. 6 and 7. Calculations of $F_{tot}(x)$ for PST (points) and partly rigid transition states with SSACM rigidity factors (full lines) in Fig. 6 gave practically the same results. On the other hand, the PST results (points) in Fig. 7 are compared with the alternative rigidity factors given above (full lines), showing that there are differences which, however, are nearly exclusively due to different $F^{sc}(x)$.

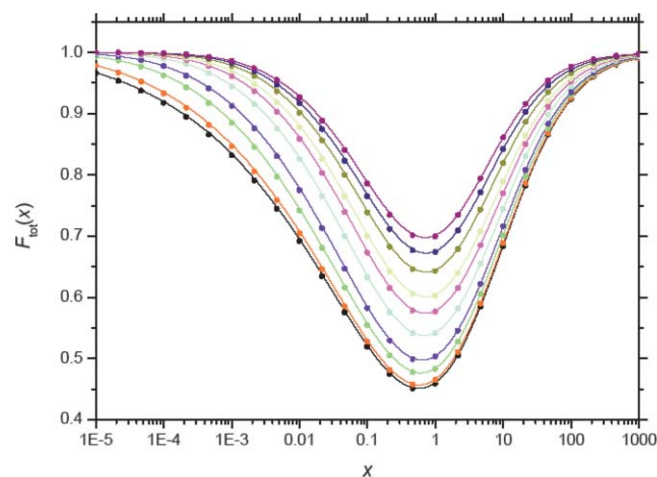


FIG. 6. Total broadening factors $F_{tot}(x)$ for the dissociation of a four-atomic molecule to atom + symmetric top fragments ($A_e/hc = 8 \text{ cm}^{-1}$, $B_e/hc = 1 \text{ cm}^{-1}$) at $T = 1000 \text{ K}$ ($E_0/hc = 30\,000 \text{ cm}^{-1}$, $F_E = 1.104$; results for $\beta_c = 0.0001, 0.001, 0.01, 0.03, 0.1, 0.2, 0.3, 0.5, 0.7$, and 0.9 from bottom to top; points = isotropic potential, i.e., phase space theory PST, lines = anisotropic potential with rigidity factors $f_{rigid}(E, J) = (1 - f_\infty) \exp[-(E - E_0(J))/c_{loose}] + f_\infty$, where $f_\infty = 0.1$ and $c_{loose}/hc = 70 \text{ cm}^{-1}$).

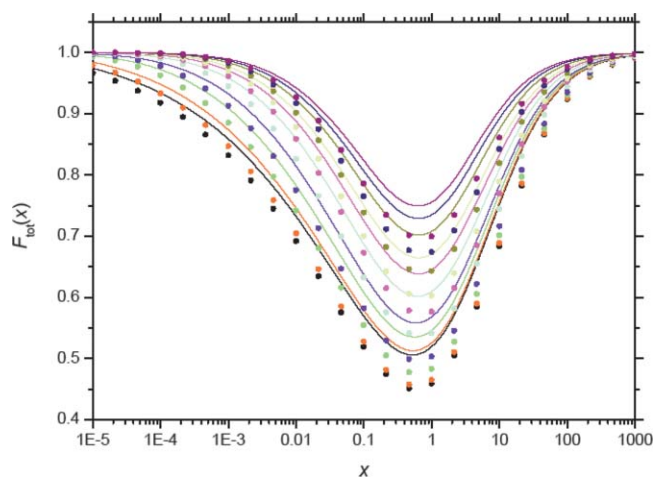


FIG. 7. As Fig. 6, but lines = anisotropic potential with rigidity factors $f_{rigid}(E, J) = \{1 + [(E - E_0(J))/c_{loose}]^2\}^{-1/2}$.

While Figs. 6 and 7 show results for atom + symmetric top fragments (with rotational constants $A_e = 8 \text{ cm}^{-1}$ and $B_e = 1 \text{ cm}^{-1}$), Fig. 8 provides PST results for $F_{tot}(x)$ for two spherical top fragments (with rotational constants $B_1 = 1 \text{ cm}^{-1}$ and $B_2 = 2 \text{ cm}^{-1}$). In this example, for small collision efficiencies $\beta_c < 0.1$, exceptionally we found some deviations between the “semiclassical,” approximate solutions of the master equation (full lines) and the accurate, numerical results (points). However, such deviations were rare, while the agreement between the two solutions usually was as good as demonstrated in Fig. 3.

The influence of the temperature on the weak collision broadening factors $F^{wc}(x)$ is documented in Figs. 9 and 10 for atom + symmetric top fragments, while Fig. 11 (corresponding to the same temperature as used in Fig. 9) compares the results for spherical top + spherical top fragments and for a larger molecular system. One recognizes some influences of the various parameters on the detailed shapes of $F^{wc}(x)$. However, in all cases one observes the same levelling of F_{cent}^{wc}

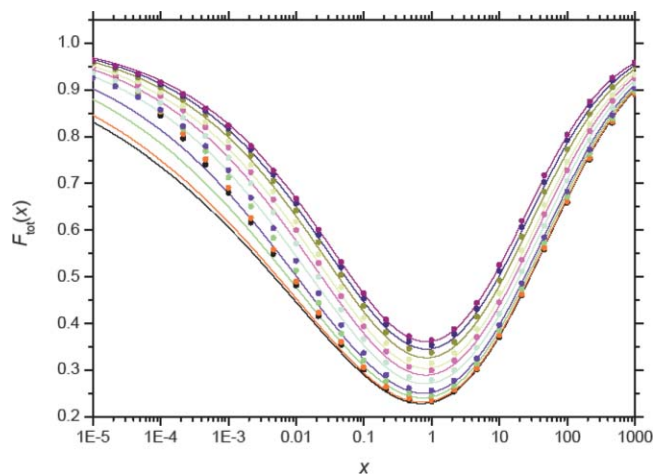


FIG. 8. Total broadening factors $F_{tot}(x)$ for the dissociation of an eight-atomic molecule to two spherical tops ($B_1/hc = 1 \text{ cm}^{-1}$, $B_2/hc = 2 \text{ cm}^{-1}$) at $T = 1000 \text{ K}$ ($E_0/hc = 30\,000 \text{ cm}^{-1}$, $F_E = 1.326$; results for β_c from bottom to top as in Figs. 6 and 7; isotropic potential, i.e., PST; lines = accurate numerical results, points = approximate “semiclassical” results).

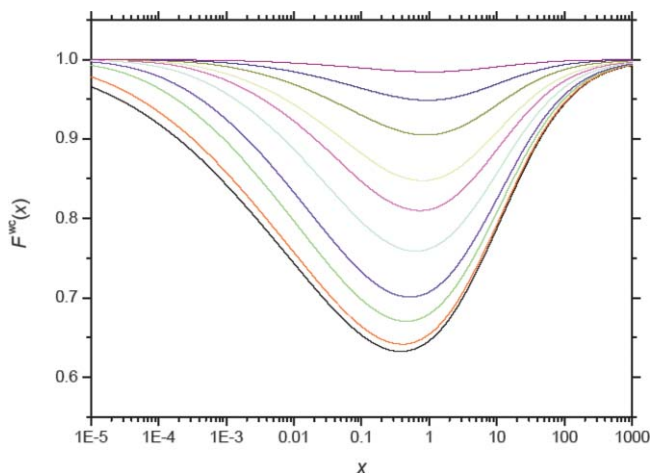


FIG. 9. Weak collision broadening factors $F^{wc}(x)$ contained in $F_{tot}(x)$ of Fig. 6 ($x = k_0/k_\infty$, $T = 1000$ K, $F_E = 1.104$; curves from bottom to top for $\beta_c = 0.0001, 0.001, 0.01, 0.03, 0.1, 0.2, 0.3, 0.5, 0.7$, and 0.9).

at small β_c as already observed in Figs. 3–5 for the model formaldehyde system. Employing the analogous representation as in Fig. 3, i.e., F_{cent}^{wc} as a function of β_c , in Fig. 12 for a selected system we compare F_{cent}^{wc} (open circles) with F_{min}^{wc} (filled circles) where the latter gives the minimum values of $F^{wc}(x)$ (the minima of the slightly asymmetric $F^{wc}(x)$ being slightly shifted from $x = 0$ to $x < 0$). We realize again that the curve for $\beta_c > 0.1$ approaches the simple law of Eq. (1.7), i.e., $F_{cent}^{wc} \approx \beta_c^{0.14}$, while it levels off with decreasing $\beta_c < 0.1$.

In order to study specificities of the dependence of F_{cent}^{wc} on β_c , in Fig. 13 we finally compare results for a series of different systems. There appears to be some spread of F_{cent}^{wc} for $\beta_c \ll 1$ around an average value of about 0.64 while the same limiting dependence of $F_{cent}^{wc} \rightarrow \beta_c^{0.14}$ is approached in all cases for $\beta_c > 0.1$. To a first approximation, this could be represented by

$$F_{cent}^{wc} \approx \max(\beta_c^{0.14}, F_{cent,0}^{wc}) \quad (5.1)$$

with $F_{cent,0}^{wc} = 0.64(\pm 0.03)$. However, one also might design more elaborate fits for the average dependence of F_{cent}^{wc} on β_c .

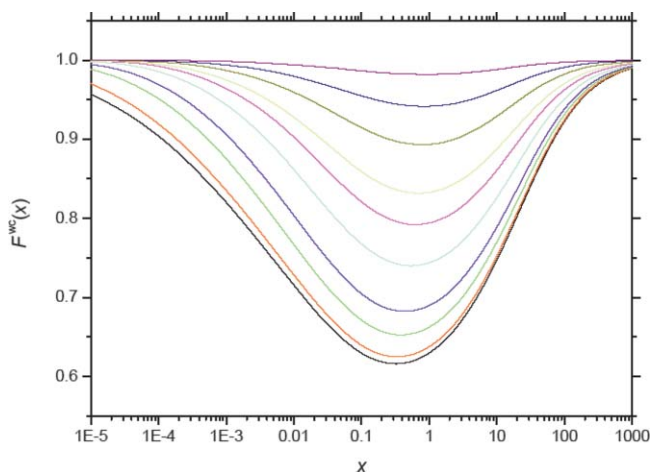


FIG. 10. As Fig. 9, but for $T = 3000$ K ($F_E = 1.370$).

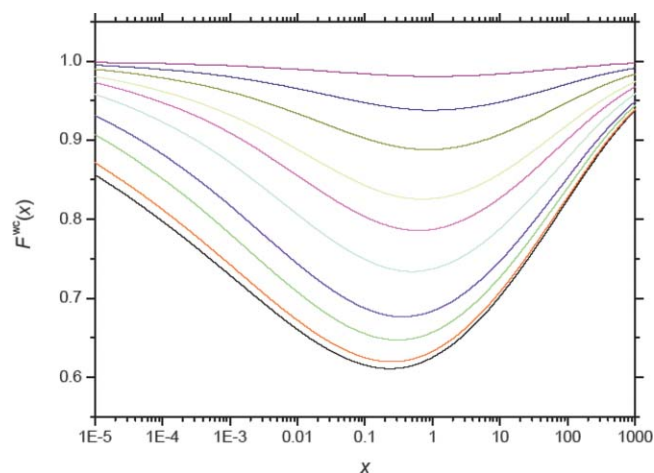


FIG. 11. Weak collision broadening factors $F^{wc}(x)$ contained in $F_{tot}(x)$ of Fig. 8 ($x = k_0/k_\infty$, $T = 1000$ K; curves from bottom to top for $\beta_c = 0.0001, 0.001, 0.01, 0.03, 0.1, 0.2, 0.3, 0.5, 0.7$, and 0.9).

VI. APPROXIMATE EXPRESSIONS FOR GENERAL BROADENING FACTORS $F(x)$

Inspecting the large number of our calculated broadening factors, parts of which were illustrated in Secs. IV and V, one observes that curves with the same F_{cent} or F_{min} nevertheless have slightly different, system-specific, shapes of the total broadening factors $F(x) = F_{tot}(x) = F^{sc}(x)F^{wc}(x)$. One, therefore, cannot hope for one, optimum, functional form of $F(x)$. At best, one can design average compromises for $F(x)$ of simpler form such as Eq. (1.5) or, if asymmetries are accounted for, of more complicated forms such as proposed in Refs. 2–15. Practical application of such expressions for $F(x)$ often shows that increasing complexity of the expression does not necessarily improve the reliability of the falloff representation. For example, a recent analysis of experimental falloff data for the recombination $2 \text{ OH} \rightarrow \text{H}_2\text{O}_2$ in Ref. 30 showed that the simple expression of Eq. (1.5) near to the center of the falloff curve within experimental scatter agreed

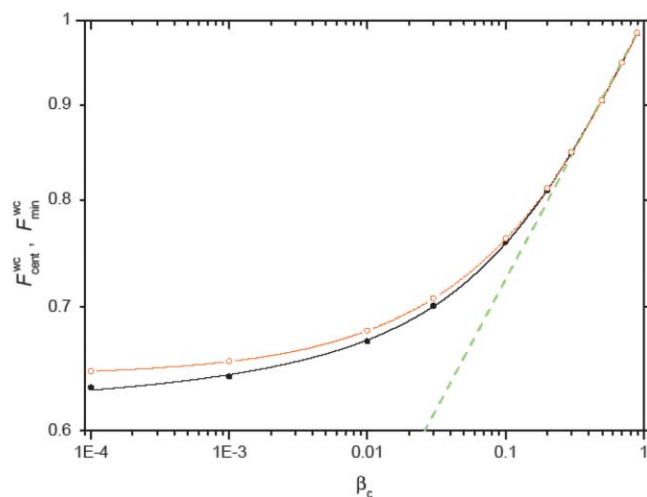


FIG. 12. Center (F_{cent}^{wc} , open circles) and minimum (F_{min}^{wc} , filled circles) weak collision broadening factors as a function of the collision efficiency β_c for the system and the conditions of Fig. 6 (the dashed line correspond to $F_{cent}^{wc} \approx \beta_c^{0.14}$ from Eq. (1.7)).

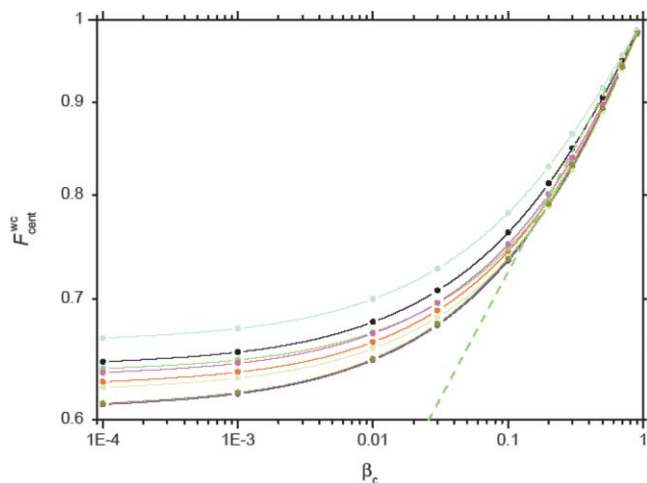


FIG. 13. Weak collision center broadening factors F_{cent}^{wc} for a variety of model systems, see text. From top to bottom: (number of atoms, products, T/K) = (4, atom + lin, 1000), (4, atom + sym top, 1000), (8, atom + sym top, 1000), (4, atom + lin, 3000), (4, atom + sym top, 3000), (8, sph top + sph top, 1000), (8, atom + sym top, 3000), (8, sph top + sph top, 3000); the last two systems nearly coincide; full lines: accurate numerical results for PST calculations, dashed line: $F_{cent}^{wc} \approx \beta_c^{0.14}$ from Eq. (1.7).

equally well with the measurements as more complicated expressions accounting for the asymmetry of the broadening factors (see Fig. 2 of Ref. 30). It, therefore, does not appear meaningful to judge the quality of new expressions for $F(x)$ on the basis of calculations for single or few reaction systems only. Real improvements will only come from accurate theoretical treatments with fully characterized specific rate constants $k(E, J)$ and collisional energy transfer probabilities $P(E', J'; E, J)$. However such calculations appear still out of reach today. Therefore, one may work with optimum compromise functions for $F_{tot}(x)$ obtained on the basis of large numbers of calculated broadening factors such as they are available in the present work. However, in order to be of use for and accepted by the kinetics community, these functions should be as simple as possible and be related to established

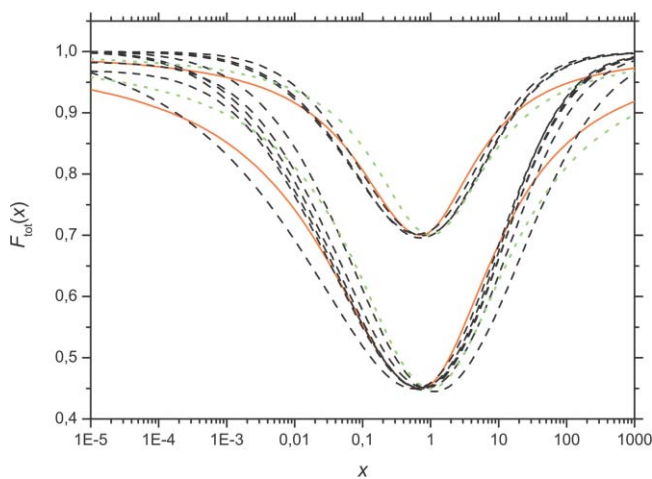


FIG. 14. Total broadening factors $F_{tot}(x)$ for a series of model systems (dashed lines, specified in the text), compared to Eqs. (1.5) and (1.6) (dotted lines) and Eq. (6.1) (full lines). Upper group of curves: $F_{cent} \approx 0.7$, lower group of curves: $F_{cent} \approx 0.45$.

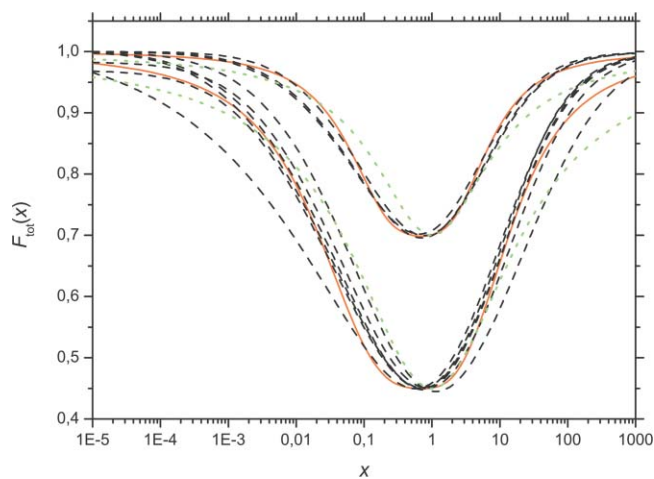


FIG. 15. As Fig. 14, but compared to Eq. (6.2) (full lines).

expressions such as given in Sec. I. For this reason, we have analyzed our calculated $F_{tot}(x)$ again, with the aim to obtain suitable expressions for asymmetric broadening factors going beyond Eq. (1.5) but being related to the general philosophy underlying this equation.

Figures 14–16 compare a selection of model functions for $F_{tot}(x)$ with a selection of calculated broadening factors from weak collision falloff curves. We have chosen two groups of examples, one for $F_{tot}(x = 1) \approx 0.7$ and one for $F_{tot}(x = 1) \approx 0.45$. All three figures correspond to model functions using the same parameters k_0 , k_∞ , and $F_{cent} = F_{tot}(x = 1)$. Figure 14 compares the calculated $F_{tot}(x)$ with the expression

$$\log F_{tot} = \log F_{cent} / \{1 + [|\log(1.4x)| / (N + \Delta N)]^2\}, \quad (6.1)$$

where $N = 0.75 - 1.27 \log F_{cent}$, $\Delta N = 0.3 \log F_{cent}$ for $\log(1.4x) > 0$ and $\Delta N = -0.7 \log F_{cent}$ for $\log(1.4x) < 0$. This expression is closest to those initially proposed in Refs. 2 and 3. Figure 15, on the other hand compares $F_{tot}(x)$ with the expression

$$\log F_{tot} = \log F_{cent} / \{1 + [|\log(1.4x)| / (N + \Delta N)]^3\}, \quad (6.2)$$

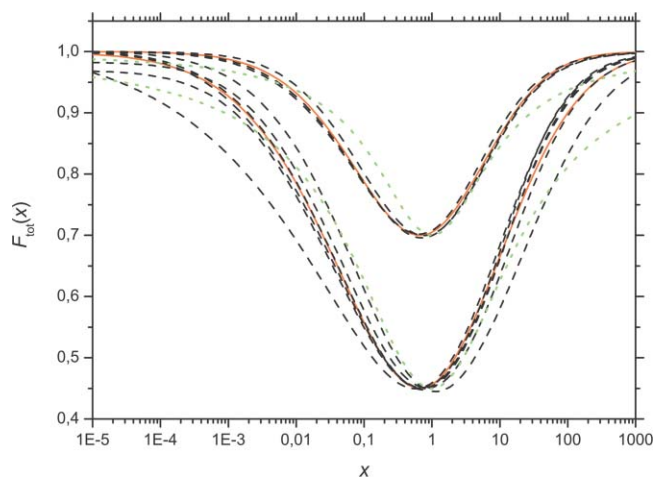


FIG. 16. As Fig. 14, but compared to Eq. (6.3) (full lines).

where $N = 0.75 - 1.27 \log F_{cent}$, $\Delta N = 0$ for $\log(1.4x) > 0$, and $\Delta N = -0.65 \log F_{cent}$ for $\log(1.4x) < 0$. Finally, Fig. 16 compares $F_{tot}(x)$ with the expression

$$F_{tot} = 1 - (1 - F_{cent}) \exp\{-[\log(1.5x)/N]^2/N^*\}, \quad (6.3)$$

where $N = 0.75 - 1.27 \log F_{cent}$, $N^* = 2$ for $\log(1.5x) > 0$, and $N^* = 2[1 - 0.15 \log(1.5x)]$ for $\log(1.5x) < 0$. The calculated broadening factors include two formaldehyde-curves with $(T/K, \beta_c, F_{cent}) = (1000, 0.08, 0.45)$ and $(3000, 0.4, 0.45)$, 4 four-atomic \rightarrow atom + top-curves with $(1000, 0.0001, 0.45)$, $(3000, 0.13, 0.45)$, $(1000, 0.9, 0.7)$, and $(1000, 0.5, 0.7)$, anisotropic rigidity factor, 2 four-atomic \rightarrow atom + linear-curves with $(3000, 0.01, 0.45)$ and $(1000, 0.27, 0.7)$, and one eight-atomic \rightarrow atom + top-curve with $(1000, 0.4, 0.45)$. The latter curve deviates from the others most at $x > 1$ whereas the four-atomic \rightarrow atom + top-curve with $\beta_c = 0.0001$ deviates most for $x < 1$. Nevertheless, the deviations of Eqs. (6.1)–(6.3) from the set of calculated broadening factors do not exceed about 10%.

The dotted lines in Figs. 14–16, for comparison, correspond to the simplest modelling expression of Eqs. (1.5) and (1.6). Although Eqs. (6.1)–(6.3) in general better account for the asymmetry of the broadening factors (i.e., broader falloff curves at $x < 1$ and narrower curves at $x > 1$), the performance of Eqs. (1.5) and (1.6) still appears satisfactory, with deviations from the band of calculated broadening factors also not exceeding more than about 10%.

VII. CONCLUSIONS

The present work, in its first part, has addressed the question to what extent weak collision broadening factors of falloff curves can be represented in a general fashion. We found that this indeed appears possible by relating the weak collision center broadening factor F_{cent}^{wc} to the weak collision efficiency β_c . Equation (5.1) in the form

$$F_{cent}^{wc} = \max\{\beta_c^{0.14}, 0.64(\pm 0.03)\} \quad (7.1)$$

was shown to provide such a general relationship. Full weak collision broadening factors $F^{wc}(x)$ were found to be of similar, but not of identical form as the total broadening factors $F_{tot}(x)$. Nevertheless, the differences turned out to be comparably small.

In the second part of this work, we compared a series of modelled total broadening factors $F_{tot}(x)$ of weak collision falloff curves with a variety of simple analytical formulae. We were interested in the question, to what extent expressions for $F_{tot}(x)$ with a minimum number of parameters can represent the general behaviour. We observed that, for a given center broadening factor $F_{tot}(x = 1) = F_{cent}$, the modelled $F_{tot}(x)$ fall within a band of about 10% width with system-specific deviations from an average curve. Modelled falloff curves of the described kind thus can be characterized by the quantities k_0 , k_∞ , and F_{cent} only to within about 10%. Nevertheless, this precision appears acceptable for most practical applications. Beyond this precision, one would need a more detailed theory which would be accurate in a variety of aspects and which presently appears out of reach.

There remains the often discussed question what would be “the best” formula to represent a falloff curve. According to the present work this question has no answer. Because of the fine details of individual reaction systems, there cannot be “one best” general expression for representing falloff curves. Instead, a variety of formulae work more or less equally well and it does not appear meaningful to prefer one over another. Ironically, the initially proposed symmetric broadening factor²

$$\log F_{tot}(x) \approx \log F_{cent} / [1 + (\log x/N)^2] \quad (7.2)$$

with $N = 0.75 - 1.27 \log F_{cent}$ on the whole still works similarly well as the more complicated asymmetric broadening factors described by Eqs. (6.1)–(6.3). Without going into more details, that applies as well to the alternatives proposed in Refs. 2–15. For this reason, there does only rarely appear a necessity to replace the well-established Eq. (7.2) by alternative expressions. In this case we recommend the use of Eq. (6.3).

A crucial point of data representation is the proper choice of F_{cent} . Whenever this is possible, it should be taken from the experimental data. When these are too limited or uncertain, unimolecular rate theory may help to estimate F_{cent}^{sc} . In addition, however, the weak collision contribution F_{cent}^{wc} should not be forgotten. It can be related to the collision efficiency β_c through Eq. (7.1). On the other hand, β_c is obtainable from an analysis of k_0 .

If F_{cent} is treated as a fit parameter for a too small part of an experimental falloff curve or if, for convenience, F_{cent} is chosen as an average standard value (e.g., $F_{cent} \approx 0.6$ such as done in Ref. 18), then one must be prepared that the values for k_0 and k_∞ deviate from the true values. This is of little relevance if only a parametrized representation of a certain part of the falloff curve is intended. However, it then may be difficult to relate the properties of the fitted k_0 and k_∞ to theoretical models of these limiting rate constants.

One final remark concerns the group of reactions considered here which are “normal” thermal unimolecular reactions and the reverse thermal recombination reactions. Tunneling effects, which lead to additional broadenings of the falloff curves at the low pressure side, have not been included, see above. Obviously, the given treatment only applies to overall rates and not to branching fractions in multi-channel dissociations or complex-forming bimolecular reactions of multi-well character. In this case, the phenomena of “rotational and vibrational channel switching” take place.³¹ Multi-well unimolecular reaction codes³² then are helpful to the extent that rotational effects can be handled realistically.

ACKNOWLEDGMENTS

Financial support of this work by the Deutsche Forschungsgemeinschaft (DFG) (Project No. TR69/18–1) is gratefully acknowledged.

¹T. Baer and W. L. Hase, *Unimolecular Reaction Dynamics. Theory and Experiments* (Oxford University Press, New York, 1996).

²J. Troe, *J. Phys. Chem.* **83**, 114 (1979).

³J. Troe, *Ber. Bunsenges. Phys. Chem.* **87**, 161 (1983).

⁴I. Oref, *J. Phys. Chem.* **93**, 3465 (1989).

- ⁵Z. Pawlowska and I. Oref, *J. Phys. Chem.* **94**, 567 (1993).
- ⁶Z. Pawlowska, W. C. Gardiner, and I. Oref, *J. Phys. Chem.* **97**, 5024 (1993).
- ⁷H. Wang and M. Frenklach, *Chem. Phys. Lett.* **205**, 271 (1993).
- ⁸A. Kazakov, H. Wang, and M. Frenklach, *J. Phys. Chem.* **98**, 10598 (1994).
- ⁹O. Prezhdo, *J. Phys. Chem.* **99**, 8633 (1995).
- ¹⁰P. K. Venkatesh, *J. Phys. Chem. A* **104**, 280 (2000).
- ¹¹C. Nyeland, *Z. Phys. Chem.* **214**, 1329 (2000).
- ¹²J. Troe and V. G. Ushakov, *Faraday Discuss.* **119**, 145 (2001).
- ¹³C. J. Cobos and J. Troe, *Z. Phys. Chem.* **217**, 1031 (2003).
- ¹⁴P. Zhang and C. K. Law, *Int. J. Chem. Kinet.* **41**, 727 (2009).
- ¹⁵P. Zhang and C. K. Law, *Int. J. Chem. Kinet.* **43**, 31 (2011).
- ¹⁶D. L. Baulch, C. T. Bowman, C. J. Cobos, R. A. Cox, T. Just, J. A. Kerr, M. J. Pilling, D. Stocker, J. Troe, W. Tsang, R. W. Walker, and J. Warnatz, *J. Phys. Chem. Ref. Data* **34**, 757 (2005).
- ¹⁷R. Atkinson, D. L. Baulch, R. A. Cox, J. N. Crowley, R. F. Hampson, R. G. Hynes, M. E. Jenkin, M. J. Rossi, J. Troe, and T. J. Wallington, *Atmos. Chem. Phys.* **8**, 4141 (2008).
- ¹⁸S. P. Sander, J. Abbatt, J. R. Barker, J. B. Burkholder, R. R. Friedl, D. M. Golden, R. E. Huie, C. E. Kolb, M. J. Kurylo, G. K. Moortgat, V. L. Orkin, and P. H. Wine, *JPL-Publication* 10-6 (JPL, Pasadena, CA, 2011).
- ¹⁹R. G. Gilbert, K. Luther, and J. Troe, *Ber. Bunsenges. Phys. Chem.* **87**, 169 (1983).
- ²⁰J. S. Poole and R. G. Gilbert, *Int. J. Chem. Kinet.* **26**, 273 (1994).
- ²¹S. C. Smith and T. J. Frankcombe, *Faraday Discuss.* **119**, 159 (2001).
- ²²J. Troe, *J. Chem. Phys.* **66**, 4745 (1977).
- ²³J. R. Barker, *Int. J. Chem. Kinet.* **33**, 232 (2001).
- ²⁴J. A. Miller, S. J. Klippenstein, S. H. Robertson, M. J. Pilling, and N. J. B. Green, *Phys. Chem. Chem. Phys.* **11**, 1128 (2009).
- ²⁵E. E. Nikitin, *Teor. Eksp. Khim* **2**, 19 (1966).
- ²⁶J. Troe and V. G. Ushakov, "SACM modeling of the three-channel dissociation of formaldehyde," *J. Chem. Phys.* (unpublished).
- ²⁷W. Forst, *J. Phys. Chem.* **87**, 4489 (1983).
- ²⁸J. Troe, V. G. Ushakov, and A. A. Viggiano, *J. Phys. Chem. A* **110**, 1491 (2006).
- ²⁹W. Stevens, B. Sztaray, N. Shuman, T. Baer, and J. Troe, *J. Phys. Chem. A* **113**, 573 (2009).
- ³⁰J. Troe, *Combust. Flame* **158**, 594 (2011).
- ³¹J. Troe, *J. Chem. Soc., Faraday Trans.* **90**, 2303 (1994).
- ³²D. M. Golden and J. R. Barker, *Combust. Flame* **158**, 602 (2011).